REPORT DOCUMENTATION PAGE

AFRL-SR-BL-TR-01-

0085

1. REPORT DATE (DD-MM-YYYY)	2. REPORT TYPE	3. DATES COVERED
22-01-2001	Final Technical	01-09-1997 - 31-08-2000

4. TITLE AND SUBTITLE
(U) Fuel-Air Mixing and Flame Structure Measurements For Advanced, Low Emission Gas Turbine Combustors

5a. CONTRACT NUMBER

5b. GRANT NUMBER
F49620-97-1-0456

5c. PROGRAM ELEMENT NUMBER
61103D

6. AUTHOR(S)
Timothy R. Frazier, Robert E. Foglesong, Robert E. Coverdill, James E. Peters, and Robert P. Lucht

5d. PROJECT NUMBER
3484

5e. TASK NUMBER
WS

5f. WORK UNIT NUMBER

7. PERFORMING ORGANIZATION NAME(S) AND ADDRESS(ES)
University of Illinois
Department of Mechanical and Industrial Engineering
1206 West Green Street
Urbana IL 61801

8. PERFORMING ORGANIZATION REPORT NUMBER

9. SPONSORING / MONITORING AGENCY NAME(S) AND ADDRESS(ES)
AFOSR/NA
801 North Randolph Street
Room 732
Arlington VA 22203-1977

10. SPONSOR/MONITOR'S ACRONYM(S)

11. SPONSOR/MONITOR'S REPORT NUMBER(S)

12. DISTRIBUTION / AVAILABILITY STATEMENT
Approved for public release; distribution is unlimited

13. SUPPLEMENTARY NOTES

14. ABSTRACT
A study of the fuel air mixing and combustion processes downstream of a dual-annular counter-rotating swirler premixer was conducted. A brief description of the facility and results from planar laser-induced fluorescence (PLIF) OH experiments and emission measurements are included in this report. OH images showed a fluctuating flame dominated by large scale structures. The flame was anchored at the edge of the premixing duct exit in the region shown in previous mixing studies to possess fuel concentrations well above the overall equivalence ratio. The area near the center of the exit of the premixer duct was almost completely devoid of reaction. Emissions measurements of NOx, CO, and UHC were also performed. NOx emissions decreased approximately 60% as equivalence ratio was decreased from 0.7 to 0.6, attributable to decreased combustion temperatures. Though combustion temperatures increased slightly for higher pressure drop conditions, NOx emissions remained constant, likely due to decreased residence times and improved mixing for the higher-pressure drops. CO emissions increased with both increasing equivalence ratio and pressure drop. In addition to OH imaging and emission measurements, coherent anti-Stokes Raman scattering measurements were used to quantify combustion temperature fluctuations.

15. SUBJECT TERMS
gas turbine, combustor, swirl, emissions, laser-induced fluorescence

16. SECURITY CLASSIFICATION OF:			17. LIMITATION OF ABSTRACT	18. NUMBER OF PAGES	19a. NAME OF RESPONSIBLE PERSON
a. REPORT	b. ABSTRACT	c. THIS PAGE			Julian M. Tishkoff
Unclassified	Unclassified	Unclassified	UL	16	19b. TELEPHONE NUMBER (include area code) (703) 696-8478

1.0 Overview

A study of the fuel/air mixing and combustion processes downstream of a dual-annular counter-rotating swirler premixer was conducted. A brief description of the facility and results from planar laser-induced fluorescence (PLIF) OH experiments and emission measurements are included in this report.

OH images show a fluctuating flame dominated by large-scale structures. The flame is anchored at the edge of the premixing duct exit in the region shown in previous mixing studies to possess fuel concentrations well above the overall equivalence ratio. The area near the center of the exit of the premixer duct is almost completely devoid of reaction.

Emissions measurements of NOx, CO, and UHC were also performed. NOx emissions decrease approximately 60% as equivalence ratio is decreased from 0.7 to 0.6, attributable to decreased combustion temperatures. Though combustion temperatures increase slightly for higher pressure drop conditions, NOx emissions remain constant, likely due to decreased residence times and improved mixing for the higher pressure drops. CO emissions increase with both equivalence ratio and pressure drop.

In addition to OH imaging and emission measurements, coherent anti-Stokes Raman scattering measurements have been used to quantify combustion temperature fluctuations.

2.0 Accomplishments

A gas turbine combustion facility with optical access that allows the use of laser diagnostic techniques to measure temperature and species concentrations within the combustion zone was used in the current study. The work presented here is part of an investigation of an aero-derivative dual annular counter-rotating swirler premixer design. Cold-flow acetone planar laser-induce fluroescence (PLIF) previously was used to investigate the mixing characteristics of this practical premixer hardware. [1, 2] The second phase of the investigation, which is presented here, includes OH PLIF and emission measurements made under atmospheric pressure combustion conditions.

2.1 Experimental Setup

2.1.1 Premixer

A schematic of the premixer that was investigated in this study is shown in Figure 1. Mixing is achieved by a dual-annular counter-rotating swirler arrangement. Ten outer vanes, which have an angle of 45°, swirl the flow clockwise (viewed from downstream) while five inner vanes at an angle of 55° rotate the inner flow counterclockwise. Gaseous fuel is introduced axially from three holes along the trailing edge of each of the outer vanes as well as radially

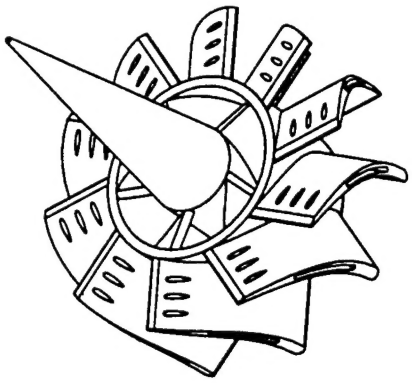

Figure 1. Dual annular counter-rotating swirler assembly as viewed from downstream.

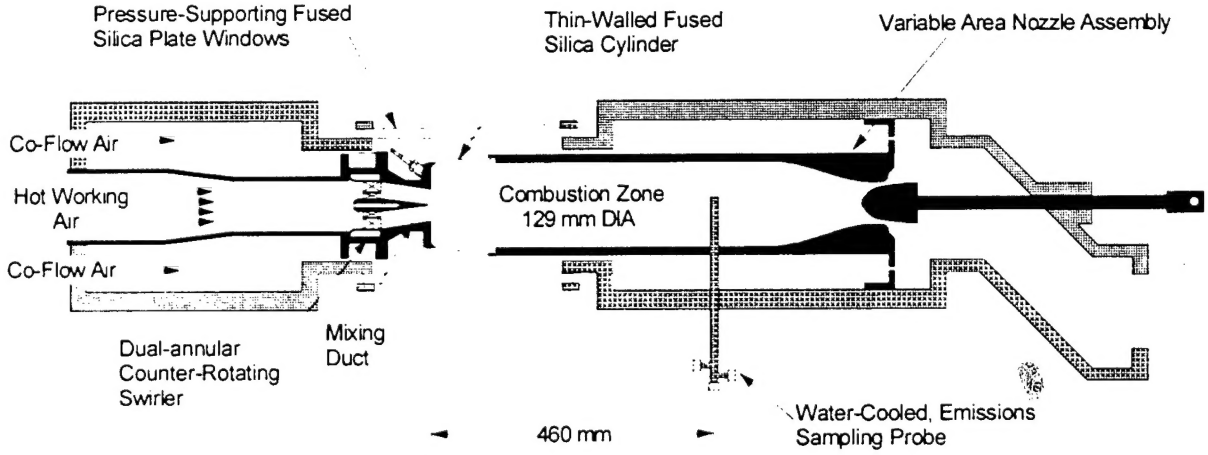

Figure 2. Schematic of experimental combustor.

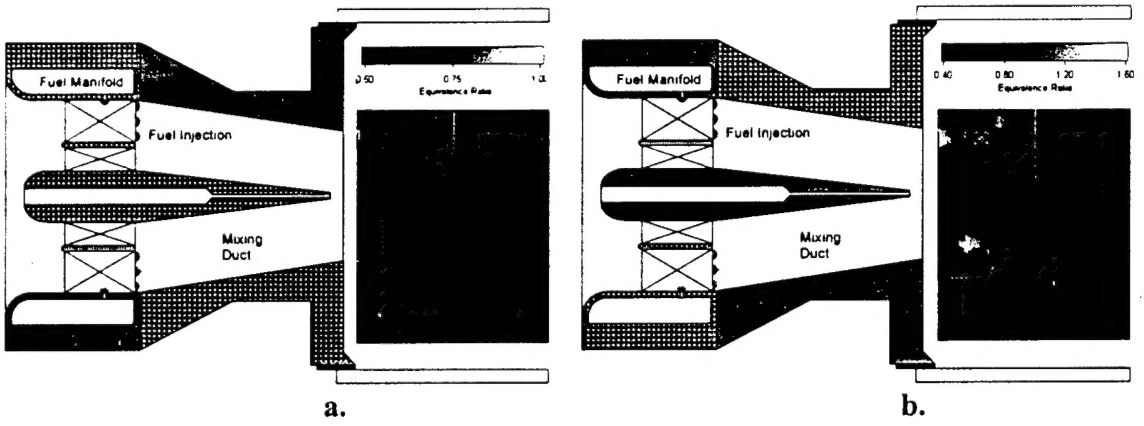

Figure 3. Representative acetone PLIF mixing images for P_{in} = 116 kPa, ΔP_{comb} = 3.2%, ϕ = 0.70, and T_{in} = 427 K; (a) time-averaged, (b) time-resolved.[12]

inward from one hole centered between each of the outer vanes. Mixing occurs within the converging section of the premixer, which can be seen in Figure 2, a schematic of the experimental combustor. The strong shear layer generated by the counter-rotating flows distributes the fuel within this converging mixing duct.

Besides aiding in fuel/air mixing, the use of the counter-rotating inner swirler helps increase the axial velocity of the flow, eliminating recirculation within the mixing duct. The 2:1 reduction in area of the mixing duct serves to continuously accelerate the flow to further increase axial velocity and minimize boundary layer thickness. These design concepts both help prevent auto-ignition and flashback within the mixing duct. The centerbody of the premixer is hollow to allow the passage of a small amount of cooling air. To prevent the flame from attaching to the centerbody tip, the centerbody does not extend to the full length of the mixing duct.[3] The diameter of the mixing duct exit is 48 mm.

Previous laser Doppler velocimetry (LDV) studies of the premixer have shown that the rotational velocity of the flow at the premixer exit is dominated by the swirl direction of the outer vanes.[2] Across the entire diameter of the exit plane of the premixing duct, the rotational velocity of the flow is in the direction of the outer vanes.

Previous acetone PLIF mixing studies have demonstrated significant non-uniformities in the fuel/air distribution produced by the premixer.[1, 2] A sample time-averaged mixing image from Frazier et al.[2] is shown in Figure 3a. For this mixing image, the flow conditions were inlet pressure, P_{in} = 116 kPa, pressure drop across the combustor, ΔP_{comb} = 3.2%, overall equivalence ratio, ϕ = 0.70, and inlet temperature, T_{in} = 427 K. (These test conditions are comparable to Test Case 1, to be introduced later in this report.) Most notable in the image are the fuel-lean central area and the fuel-rich annulus around the edge of the premixer exit. For this ϕ = 0.7 test case, time-averaged equivalence ratios are near 0.5 in the central region. Near the edge of the premixer exit, time-averaged equivalence ratios reach 1.05, or 50% above the overall equivalence ratio of the combustor.

Time-resolved mixing images reveal large scale structures that dominate the mixing field. A representative time-resolved mixing image is shown in Figure 3b. Time-resolved measurements indicate equivalence ratios that far exceed those seen in time averaged results. For the conditions corresponding to Figure 3, local equivalence ratios as high as 1.71 were seen on a time-resolved basis.[1]

2.1.2 Combustor

As shown in Figure 2, the fuel/air mixture is dumped from the mixing duct into the cylindrical combustion zone across a 7.2:1 expansion. To provide optical access for laser diagnostic measurements, a 101-mm-long, thin-walled fused silica cylinder serves as the combustor wall immediately downstream of the premixer. Due to the complicated sealing

around the cylinder, this provides for approximately 76 mm of optical access along the length of the combustor. To minimize the pressure containment requirements of this thin-walled cylinder, the inner pressure of the combustor is matched by cold co-flow air, which also serves to cool the outer wall of the combustor.

The flow is unobstructed downstream of the premixer exit for a distance of approximately 3.5 combustor diameters (460 mm). Here, a water-cooled emissions sampling probe collects combustion product gases for measurement of CO, NO/NO_x, O_2, CO_2, and unburned hydrocarbon (UHC) concentrations. The sampling probe can be traversed radially across the entire combustor diameter.

Past the sampling probe, the combustion flow enters a converging axisymmetric nozzle, which provides for control of the pressure drop across the combustor and, hence, the mass flow rate through the combustor. At high combustor operating pressure conditions, this axisymmetric nozzle also serves to choke the flow, preventing disturbances generated in the exhaust section from propagating upstream.

The combustion facility is capable of supplying high-pressure (up to 650 kPa), high-temperature (up to 760 K) air to the premixer. The premixer is fueled by commercial grade methane. The flow control is performed by a LabVIEW driven data acquisition system. Additional information about the combustion facility can be found in Reference 1.

2.1.3 OH PLIF System

For the OH PLIF measurements, the overlapping $Q_2(8)$ and $Q_1(9)$ lines of the (1,0) vibrational band of the $A^2\Sigma$-$X^2\Pi$ system of OH are excited. This combination of lines provides strong absorption and therefore yields high fluorescence signals. The frequency-doubled output of a ND:YAG laser (Continuum PL-8010) pumps a narrowband dye laser (Continuum ND-6000) using Rhodamine 590 dye dissolved in methanol. The output of the dye laser is frequency doubled using an Inrad Autotracker III to generate the 283.92 nm excitation laser radiation.

A spherical/cylindrical lens system generates a laser sheet of approximately 45 mm in width. A 105-mm UV lens captures the fluorescence signal from the (1,1) and (0,0) bands around 310 nm with a 240x512 pixel intensified CCD camera. Because the wavelengths of the fluorescence signal are far from the wavelength of the excitation laser, elastically scattered laser light can easily be removed via filters. For this purpose, a Schott WG-305 long pass filter is used. A Schott UG-11 band pass filter is also employed to further reduce scattered laser light, as well as block flame luminescence and reduce visible fluorescence from the fused silica cylinder. The images from the 8-bit camera are reported in gray scale values from 0 to 255.

The sheet-forming optics and acquisition system are mounted on a stage that can be translated along the axis of the combustor, so that the multiple regions along the length of the combustor are accessible. The 45 mm width of the laser sheet allows the entire axial distance,

76 mm, of the visible area of the combustor to be imaged with two axial laser locations as shown in Figure 4. However, due to thermal expansion of the test section during the experiments, the axial length of the imaged region was reduced to approximately 63 mm. A lip on the edge of the backface of the combustor, which is used to aid in sealing the upstream edge of the fused silica cylinder, allows imaging only as close as 5 mm from the premixer exit.

The optimum combination of resolution and field of view is obtained by positioning the camera to capture an approximately 80 mm section of the beam sheet, extending from 50 mm to the beam entry side of the centerline to 30 mm on the other side. This field of view allows the symmetry of the premixer exit to be captured as well as a significant portion of the recirculation zone outside the premixer edge. With this configuration, the rectangular pixels of the intensified CCD camera provide a resolution of 0.17 mm/pixel in the radial direction and 0.27 mm/pixel in the axial direction.

A reference image, which would account for non-uniformities in the beam profile, was not obtained. Some normalization can be performed based on the overlap of the two image areas using the time-averaged OH PLIF images. This allows the relatively uniform upstream edge of the laser sheet to normalize the downstream edge of the laser sheet, which at its edge trails off to approximately 50% of the peak sheet intensity. In addition, shot-to-shot variations in laser power are not corrected.

The laser can be redirected to a reference burner during the experiment. This system generates an LIF signal that is captured by a BOXCAR-integrated photomultiplier tube. This signal allows the frequency doubled dye laser to be quickly and precisely tuned on and off the LIF resonance during the experiment, allowing off-resonance images to be captured at each operating condition.

2.1.4 Test Conditions

Prior to performing the experiments, shake-down combustion tests were used to identify a number of performance characteristics of the combustor. This experience aided in the selection of the test matrix. For ignition and stable combustion at the lean equivalence ratios investigated here, the combustor requires an inlet temperature of above 500 K. Through the course of the experiments, temperatures were therefore maintained above this level, varying between 540 K and 615 K. Lean blowout (LBO) was found to occur at an equivalence ratio of approximately 0.55. To prevent accidental blowout of the flame the minimum equivalence ratio studied for these tests was approximately 0.60.

For comparison with the previous mixing studies[1, 2] a similar set of test conditions was used. For these approximately atmospheric pressure combustion studies, four combinations of equivalence ratio (nominally 0.6 and 0.7) and pressure drop across the combustor (nominally 3% and 5%) were investigated. The actual run conditions for the four cases are listed in Table 1.

Table 1. Test case operating conditions and sampling probe measurements (± indicates minimum and maximum observed values).

Test Case	P_{in} (kPa)	ΔP_{comb} (%)	ϕ	T_{in} (K)	[CO] (ppm)	[NO_x] (ppm)	$T_{exhaust}$ (K)
1	113.4 ±3.2	3.0 ±0.2	0.69 ±0.02	575 ±12	76.9 ±28.6	9.3 ±1.3	1430 ±13
2	113.4 ±3.3	3.1 ±0.3	0.61 ±0.01	604 ±12	26.4 ±9.7	3.5 ±0.3	1367 ±4
3	115.1 ±1.2	4.8 ±0.3	0.70 ±0.02	564 ±25	118.6 ±41.2	8.0 ±1.4	1446 ±16
4	114.2 ±.0.7	5.1 ±0.2	0.60 ±0.02	592 ±12	53.1 ±20.9	3.8 ±0.9	1378 ±19

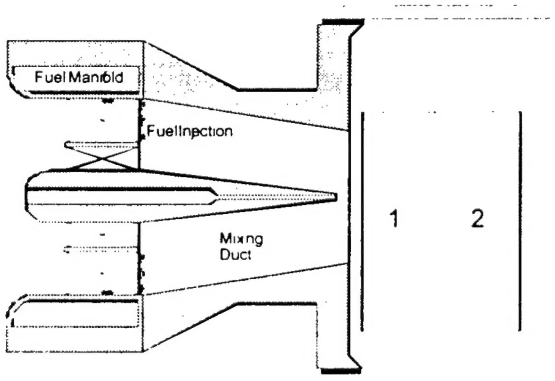

Figure 4. Image regions for OH PLIF.

Emissions sampling was performed at each test condition simultaneously with the OH PLIF measurements. Radial sweeps of the sampling probe were also performed to determine the uniformity of the product gas composition at the axial location of the emissions probe. A thermocouple mounted on the emissions probe was used to measure exhaust temperature at the various flow conditions.

2.2 Results and Discussion

2.2.1 Time-Resolved OH PLIF Imaging

The OH PLIF results provide a great deal of insight into this practical combustion system. Figures 5, 6, and 7 show series of temporally-resolved OH PLIF image assemblies for test cases 1, 2, and 3, respectively. Background and noise signal levels in these images are extremely low. Off-resonance images, aside from local regions of fluorescence of the fused silica cylinder,

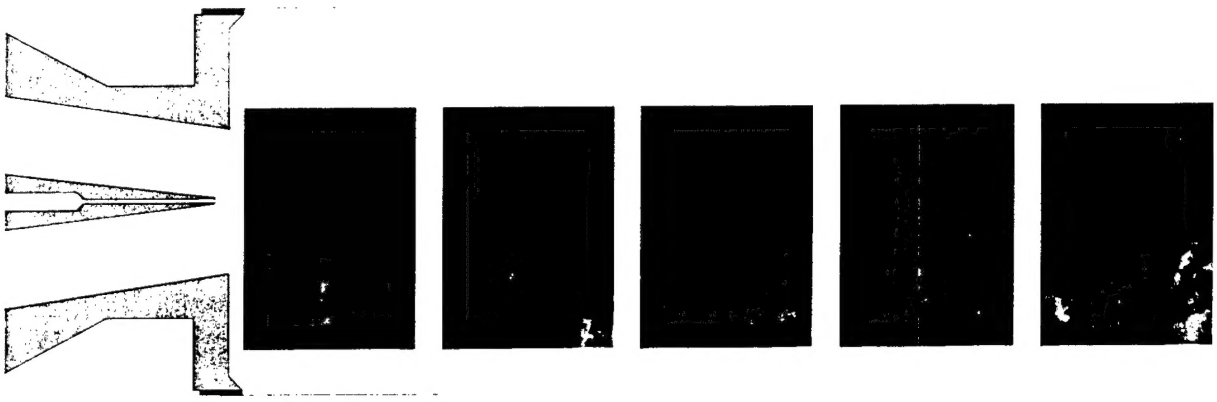

Figure 5. Series of five time resolved OH PLIF image assemblies (regions 1 and 2) for Test Case 1: P_{in} = 113 kPa, ΔP_{comb} = 3.0%, ϕ = 0.69, and T_{in} = 575 K.

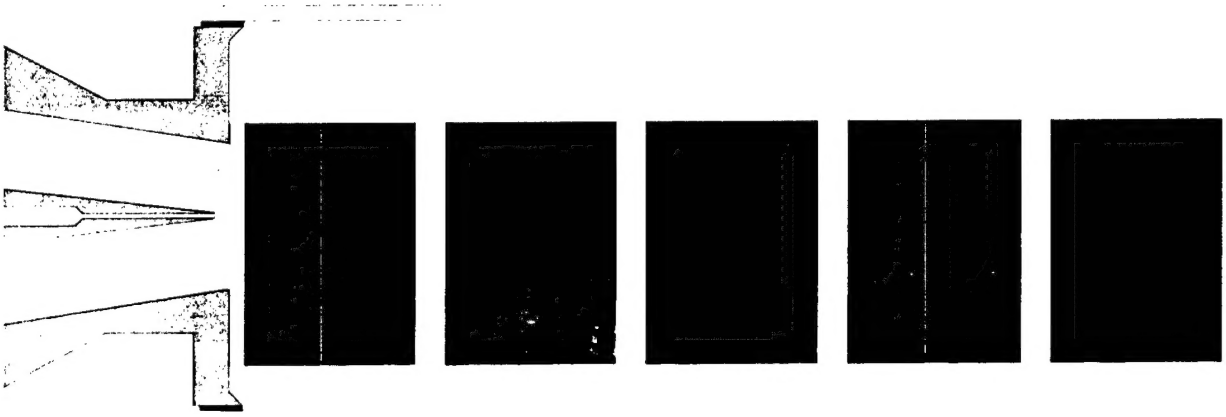

Figure 6. Series of five time resolved OH PLIF image assemblies (regions 1 and 2) for Test Case 2: P_{in} = 113 kPa, ΔP_{comb} = 3.1%, ϕ = 0.61, and T_{in} = 604 K.

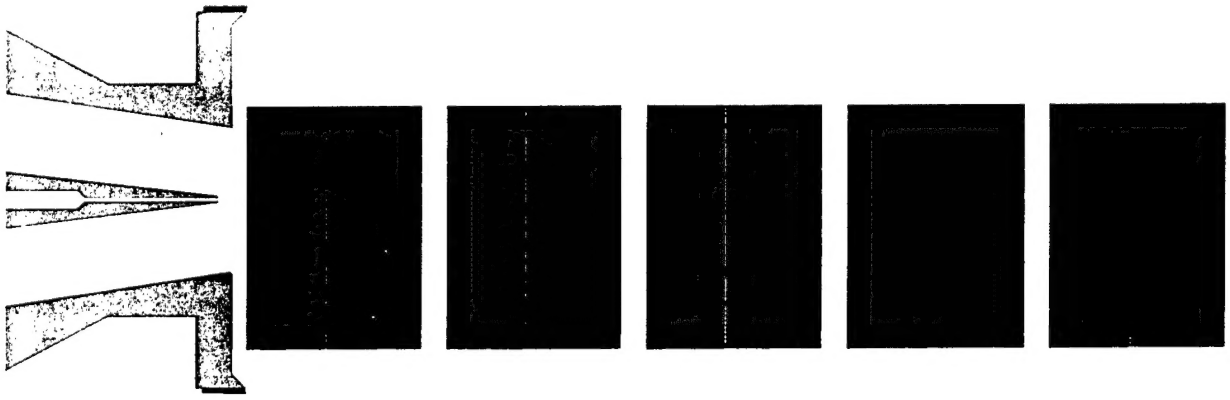

Figure 7. Series of five time resolved OH PLIF image assemblies (regions 1 and 2) for Test Case 3: P_{in} = 115 kPa, ΔP_{comb} = 4.8%, ϕ = 0.70, and T_{in} = 564 K.

showed background levels, including camera noise, flame luminescence, and laser scattering, on the order of only zero to one counts, compared to peak OH signals of up to 240 counts.

From the time-resolved images, a number of characteristics about the combustion flowfield can be identified. Most obvious is that, as evidenced by the previous mixing studies, the flowfield is dominated by large scale structures, with significant temporal variations occurring in these structures. Often they can be seen separating, creating isolated flame pockets.

Second, one notices the void along the center of the combustor. At the outside of this void, the high gradient in the OH fluorescence signal levels indicate the location of the reaction zone, which is clearly anchored at the edge of the premixer. The radial position of the reaction zone oscillates and occasionally, towards the downstream edge of the images, the edge of the reacting zone can be seen closing inward as the vortex generated by the premixer swirlers breaks down.

From the time-resolved images, little difference can be seen in the shapes of the flame zone for the different operating conditions. Signal intensities do, however, change between the test cases. These changes can be better identified and explained by examining time-averaged PLIF images.

2.2.2 Time-Averaged OH PLIF Imaging

Figures 8, 9, and 10 show time-averaged PLIF image assemblies for test conditions 1, 2, and 3, respectively. Each image is an average of 240 laser shots. The intensities of the time-averaged images were increased by 50%, relative to the intensities shown in the temporally resolved images, to improve contrast. Above each image are line plots showing averages and standard deviations of signal level at three axial locations—6 mm, 34 mm, and 61 mm downstream of the premixer exit.

A number of similar traits can be seen in the images and line profiles at all three operating conditions presented. At the farthest upstream location, 6 mm from the premixer exit, one can clearly discern the anchoring of the flame to the edge of the mixing duct exit. At this axial location, within the region radially confined by the premixer edge, there is very little OH signal present. At the premixer edge, the sharp rise in OH concentration indicates the average location of the reaction zone (note: the isolated peaks are due to reflections on the fused silica cylinder). OH signal levels slowly trail off towards the edge of the combustor in the recirculation zone formed in the corner of this dump region. It is unclear whether the OH signals from this recirculation zone are due to the occurrence of flame reactions there or due to OH molecules persisting in the product gases convecting into this area.

Within the 12 mm radius around the centerline of the premixer exit, zero OH fluorescence was detected. Between 12 mm and 24 mm from the centerline of the premixer exit, low OH signal levels are seen in the average profiles. These low average signals are not due to the occasional presence of reaction in this region. Standard deviations of OH concentration in this

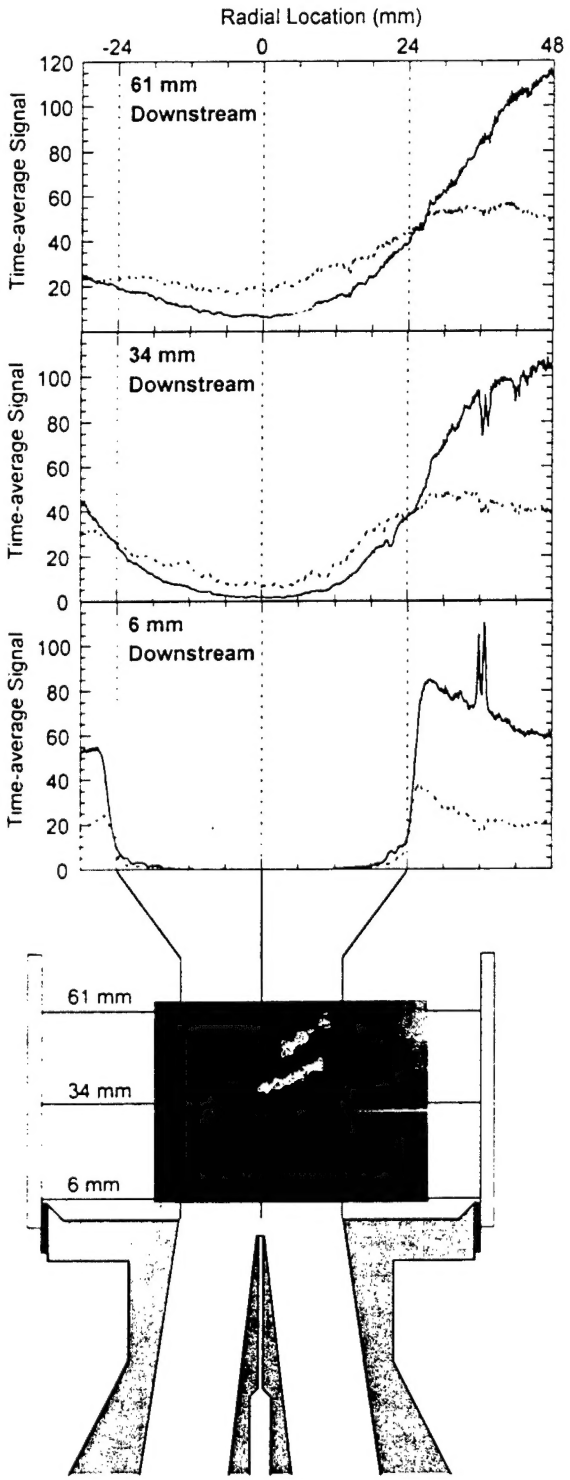

Figure 8. Time-averaged (240 shots) OH PLIF image assembly (regions 1 and 2) along with line averages of signal level at three axial locations, Test Case 1: P_{in} = 113 kPa, ΔP_{comb} = 3.0%, ϕ = 0.69, and T_{in} = 575 K. The solid line represents average signal; the dotted line represents standard deviation in signal.

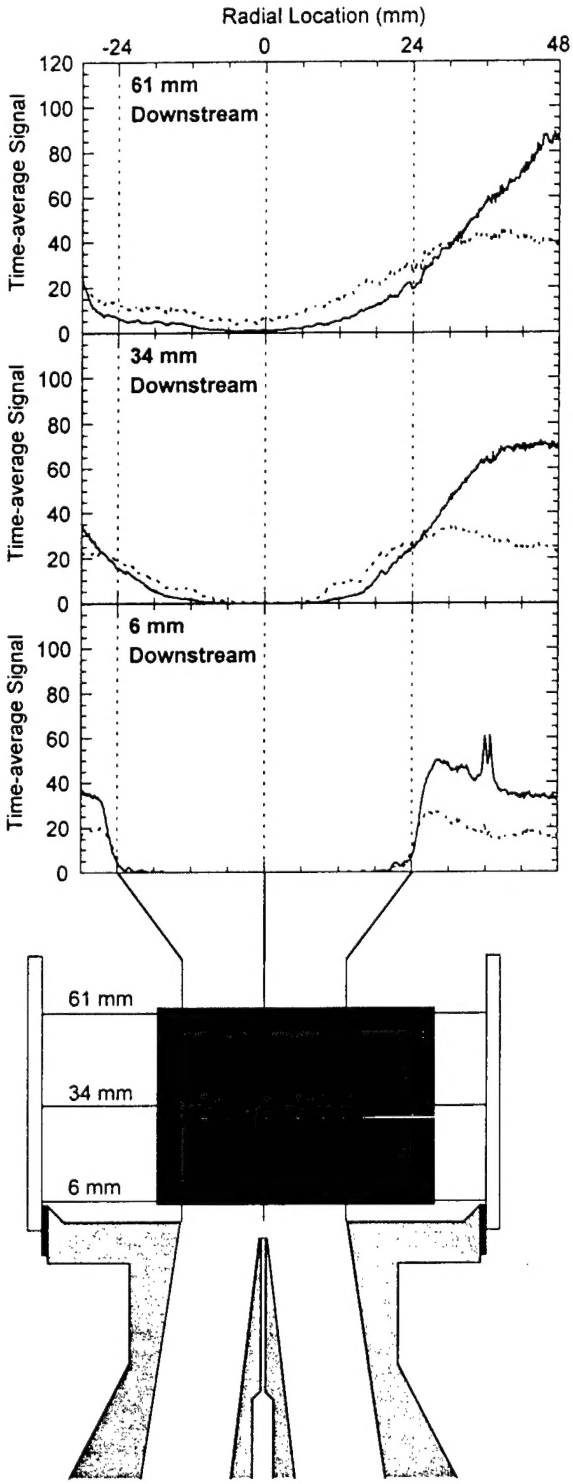

Figure 9. Time-averaged (240 shots) OH PLIF image assembly (regions 1 and 2) along with line averages of signal level at three axial locations, Test Case 2: P_{in} = 113 kPa, ΔP_{comb} = 3.1%, ϕ = 0.61, and T_{in} = 604 K. The solid line represents average signal; the dotted line represents standard deviation in signal.

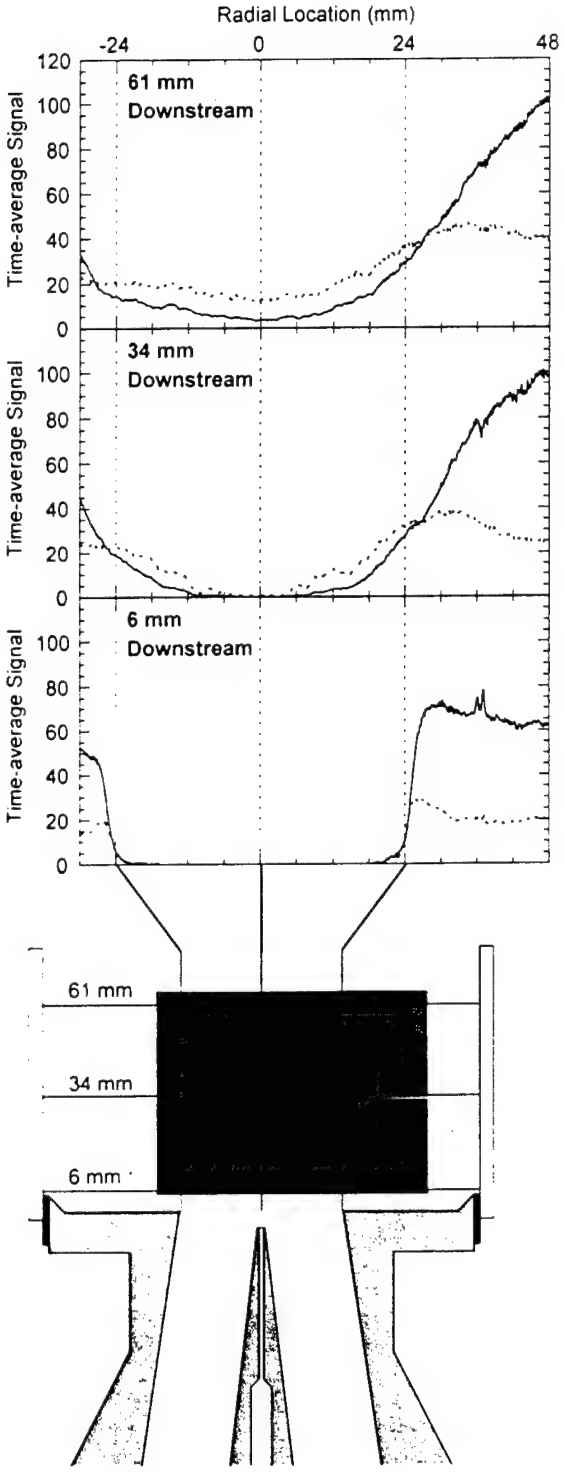

Figure 10. Time-averaged (240 shots) OH PLIF image assembly (regions 1 and 2) along with line averages of signal level at three axial locations, Test Case 3: P_{in} = 115 kPa, ΔP_{comb} = 4.8%, ϕ = 0.70, and T_{in} = 564 K. The solid line represents average signal; the dotted line represents standard deviation in signal.

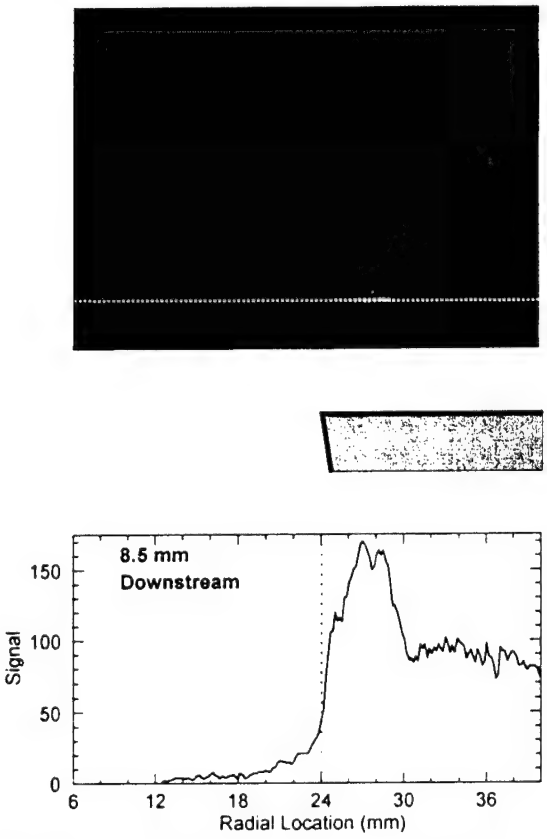

Figure 11. (a) Blow-up of the exit region in Image 1 of Figure 5. (b) Line profile of OH signal at 8.5 mm downstream as marked by dotted line in (a).

region are very low. These low signal level areas can, in fact, consistently be seen along the inner edge of the reaction zone in temporally-resolved measurements. Figure 11a is an expanded view of the exit region for the first of the five images shown in Figure 5. Figure 11b is a line profile from this region and clearly shows the presence of this low signal region along the inner edge of the reaction zone. In fact, this area of low OH concentration is nearly always present along the entire length of the combustion zone.

Moving downstream to 34 mm from the premixer exit, the OH signal profile has smoothed considerably. Intermittent oscillations of the flame front, which can be clearly seen in the temporally resolved images in Figures 5, 6, and 7, have begun to elevate average OH signal levels in the central portion of the combustor. Peak average signal levels have also expanded radially outward.

Farther downstream at 61 mm from the premixer exit, the farthest downstream location captured in the images, the time-averaged signal profiles are more uniform still. Greater time-average signals are seen in the center of the combustor, an indication of the more frequent collapse in this region of the vortex created by the premixer flow. The standard deviation in signal intensity, which exceeds the average signal level significantly, is a further indicator of the large temporal fluctuations in the flow at this location. Peak OH concentrations have been pushed still further outward.

Comparing the time-averaged profiles of test cases 1 and 3, one finds two notable differences. First, near the premixer exit, there is a less distinct peak in OH levels near the combustor edge for the 5% case. This change can be explained by trends found in the mixing studies, which showed that mixing was improved—maximum single-shot and average local equivalence ratios were decreased—for the 5% pressure drop case [1] These lower local equivalence ratios would indeed lead to decreased peak OH concentrations.

Downstream at the 34 mm and 61 mm locations, we also find that for the 5% pressure drop the low signal level region in the average profile is measurably wider than for the 3% test case. Also, for the 5% pressure drop cases, average OH signal levels are lower near the center of the combustor. This can be explained by the greater bulk flow velocity of the reactants in the 5% pressure drop case which would tend to expand the average flame location both downstream and outward, leaving this larger uncombusted void in the center.

Overall signal levels found in the $\phi = 0.6$ tests are lower than those in the $\phi = 0.7$. This result is expected in view of known trends in adiabatic equilibrium OH concentrations with decreasing equivalence ratio.

Finally, study of the time-averaged line profiles indicates significant attenuation of the beam (the beam passes from right to left). Both the $Q_2(8)$ and $Q_1(9)$ lines are strong absorbers. Unfortunately, this is an unavoidable tradeoff which must be accepted in order to obtain high

signal levels. Additional information can, however, be gained from the level of attenuation of the excitation laser. The amount of attenuation in the laser will be proportional to the total cumulative concentration of OH along the path of the laser. The greatest attenuation occurs downstream, indicating that greater total quantities of OH at these downstream locations. This would suggest that combustion is still taking place at these downstream locations and the OH in these regions has not simply been swept there from upstream.

2.2.3 Comparison of OH PLIF and Mixing Measurements

Comparing the OH PLIF images to the typical acetone PLIF mixing images shown in Figure 3 provides additional insight into the character of the combustion flowfield. The most obvious comparison is the correspondence between the high equivalence ratio annulus around the outer edge of the premixer exit and the anchoring of the flame at this same position. Also, the flame is almost entirely absent from the central region of the flow where average equivalence ratios fall well below the overall equivalence ratio of the flow.

While this clearly makes for an interesting comparison, the location of the reaction zone at the edge of the premixer is not necessarily due to the presence of the high equivalence ratios there. It would be expected that the flame would naturally anchor itself in this high shear region where the high speed flow expelled from the combustor interacts with the low speed recirculation zone. The low velocity boundary layer formed on the outer wall of the mixing duct would also lead to the anchoring of the flame at this point.

Similarly, one would not expect a great deal of combustion to take place near the center of the premixer exit. To prevent flashback, the high speed fuel/air mixture in the mixing duct flows at a rate much greater than the flame's propagation velocity. Thus, after the flow exits the mixing duct, it must slow considerably before it approaches the flame propagation velocity. For this flow, some deceleration occurs to the expansion into the dump combustor. However, the primary mechanism that determines the location where the reaction front closes is vortex breakdown, which begins to occur several centimeters downstream of the premixer exit.

What is clear in these comparisons is that a great deal of the reaction is occurring in the high-equivalence-ratio zones identified by the mixing studies, which is clearly not optimum with respect to the goal of minimizing NO_x generation.

2.2.4 Emission Results

Radial sweeps of the emissions probe showed emissions were uniform across the diameter of the combustor at the sampling probe's downstream location. Equivalence ratios back calculated from emissions measurements using the method suggested by Spindt[4] were within 4% of equivalence ratios based on air and fuel mass flow rates. NO_x and CO emissions data are presented in Table 1. For all test conditions, UHC levels were below the measurable limits of the HC analyzer system (<1-2 ppm).

As expected, reductions in equivalence ratio lead to a clear reduction in NO_x emissions, which are corrected to 15% oxygen dry. As equivalence ratios drop from 0.7 to 0.6, NO_x emissions decrease from approximately 8-9 ppm to 3-4 ppm. Changes in pressure drop lead to very little change in NO_x emissions.

Fluctuations in CO emissions were significant although trends in average CO emissions data are still evident as seen in Table 1. Decreasing equivalence ratio can be expected to cause decreasing CO emissions based on adiabatic flame equilibrium concentrations. However, as equivalence ratios approach LBO conditions, local quenching can lead to increased CO generation. As stated previously, LBO for this combustor has been found to occur at an equivalence ratio of approximately 0.55. The minimum equivalence ratio studied here, approximately 0.60, is not yet in this LBO regime. Decreases in equivalence ratio from 0.70 to 0.60, between tests cases 1 and 2 and test cases 3 and 4, led to over 50% reductions in CO emissions.

Increases in pressure drop led to significantly increased CO emissions for both equivalence ratios. The decreased residence times for the 5% pressure drop cases can be expected to increase CO emissions compared to the 3% pressure drop cases. A second possibility for the increased CO levels at 5% pressure drop is the quenching of the combustion reactions by the water-cooled combustor walls. As shown in the OH PLIF measurements, the 5% pressure drop test conditions expand the flame outward radially. If a significant portion of the reaction is occurring past the downstream edge of the fused silica cylinder, additional CO could be generated due to increased quenching from the water-cooled walls.

2.3 Conclusions

OH PLIF measurements were performed in the combustion zone of an experimental dual-annular counter-rotating swirler premixed gas turbine combustor. Images showed a fluctuating flame dominated by large scale structures. The flame was anchored at the edge of the premixing duct exit in the region shown in previous mixing studies to possess fuel concentrations well above the overall equivalence ratio. The area near the center of the exit of the premixer duct was found to be almost completely devoid of reaction.

Emissions measurements of NO_x, CO, and UHC were also performed. NO_x emissions decreased approximately 60% as equivalence ratio was decreased from 0.7 to 0.6, attributable to decreased combustion temperatures. Though combustion temperatures increased slightly for higher pressure drop conditions, NO_x emissions remained constant, likely due to decreased residence times and improved mixing for the higher pressure drops. CO emissions increased with both equivalence ratio and pressure drop.

Additional experiments are planned for this dual-annular counter-rotating swirler. Further OH PLIF and emissions measurements will be made at elevated pressures. Coherent anti-Stokes Raman scattering measurements will then be performed in the reaction zone to analyze temporal fluctuations in temperature, which will provide additional insight into the formation of NO_x in this system.

2.4 References

1. Frazier, T. R., Foglesong, R. E., Coverdill, R. E., Peters, J. E., and Lucht, R. P., "An Experimental Investigation of Fuel/Air Mixing in an Optically Accessible Axial Premixer," AIAA Paper 98-3543, July 1998.
2. Frazier, T. R., Foglesong, R. E., Coverdill, R. E., Peters, J. E., and Lucht, R. P., "Fuel/Air Mixing Measurements in a Lean Premixed Gas Turbine Combustor," to be submitted for publication to *ASME Journal of Engineering for Gas Turbines and Power*, 1999.
3. Joshi, N. D., Epstein, M. J., Durlak, S., Marakovits, S., and Sabla, P. E., "Development of a Fuel Air Premixer for Aero-Derivative Dry Low Emissions Combustors," ASME Paper 94-GT-253, June 1994.
4. Spindt, R. S., "Air-Fuel Ratios from Exhaust Gas Analysis," SAE Paper 650507, 1965.

3.0 Personnel

The AASERT program supports Timothy R. Frazier, a Ph.D. candidate and John J. Stephens, an undergraduate. Two other graduate students, Robert E. Foglesong and Luis M. Flamand, are also associated with the research effort. The co-principle investigators on the project are Professor James E. Peters and Professor Robert P. Lucht.

4.0 Publications

Foglesong, Robert E., Timothy R. Frazier, Luis M. Flamand, James E. Peters, and Robert P. Lucht, "Flame Structure and Emissions Characteristics of a Lean Premixed Gas Turbine Combustor," presented at the 35th AIAA/ASME/SAE/ASEE Joint Propulsion Conference and Exhibit, June 20-24, 1999, Los Angeles, California.

5.0 Interactions/Transitions

No interaction or transitions took place during the reporting period of August 1, 1998 to July 31, 1999.

6.0 Discoveries, inventions and/or disclosures

There were no discoveries, inventions or patent disclosures during the reporting period of August 1, 1998 to July 31, 1999.

7.0 Honors/Awards

R.P. Lucht was named an Associated Fellow of the OSA in 1998. J.E. Peters was named an Associated Fellow of the AIAA in 1991 and a Fellow of ASME in 1997.